

# Exo-anomeric effects on energies and geometries of different conformations of glucose and related systems in the gas phase and aqueous solution

Christopher J. Cramer <sup>a,\*</sup>, Donald G. Truhlar <sup>a</sup>, Alfred D. French <sup>b</sup>

<sup>a</sup> *Department of Chemistry and Supercomputer Institute, 207 Pleasant St. SE, Minneapolis, MN 55455-0431, USA*

<sup>b</sup> *United States Department of Agriculture, Agricultural Research Service, 1100 Robert E. Lee Blvd., P.O. Box 19687, New Orleans, LA 70179-0687, USA*

Received 1 July 1996; accepted 30 October 1996

## Abstract

Ab initio calculations predict that in 2-hydroxy- and 2-methoxytetrahydropyran, hyperconjugative delocalization of lone-pair density on the exocyclic oxygen atom at C-1 into the  $\sigma^*$  orbital of the C-1–O-5 bond is maximized when the OR group at C-1 is oriented gauche to C-1–O-5. This exo-anomeric effect lengthens the C-1–O-5 bond, shortens the exocyclic C-1–O bond, and stabilizes the gauche conformers by about 4 kcal/mol over the anti. In the anti orientation, hyperconjugative interaction of the OR group at C-1 with other appropriately oriented  $\sigma^*$  orbitals increases, but the geometric and energetic consequences are less marked. Solvation effects reduce the energetic stabilization associated with the exo-anomeric effect in the tetrahydropyrans. This derives from a combination of changes in the overall electrostatics and also from decreased accessibility of the hydrophilic groups in the gauche conformers. For glucose or glucosides, instead of the simple tetrahydropyran model systems, the interactions of the exocyclic OR group at C-1 with the hydroxy group at C-2 can significantly affect these hyperconjugative delocalizations. In the glucose and glucoside systems, solvation effects oppose the formation of intramolecular hydrogen bonds. MM3(94) force field calculations show systematic deviations in the relative energies and structures of the various model systems with respect to the more reliable HF/cc-pVDZ predictions. © 1997 Elsevier Science Ltd. All rights reserved.

**Keywords:** exo-Anomeric effect; Hyperconjugation; Conformational analysis; Solvation

\* Corresponding author.

## 1. Introduction

The term ‘anomeric effect’ was originally applied to describe the unexpected stability of pyranose and pyranoside structures with axial substituents at the anomeric, i.e., C-1, position (Scheme 1) [1–7]. This effect has been rationalized as arising from decreased dipole–dipole repulsion between C–O bonds in the axial anomer [8–10] and/or from greater hyperconjugative stabilization of pyranose oxygen lone-pair density when delocalized into the empty axial  $\sigma_{\text{CO}}^*$  orbital [11–14] (Fig. 1). The degree to which these two phenomena contribute in any given system (or the degree to which it is profitable to single out either of these two explanations for the single physical effect) depends on the molecular structure [5,15–23] and the surrounding medium [5,7,17,24–36].

The term anomeric effect has subsequently also been used to refer to other features of pyranoses axially substituted at the anomeric position. In particular, certain geometric features that are consistent with the above-noted hyperconjugative delocalization are observed: the C-1–O-1 bond is lengthened, the C-1–O-5 bond is shortened, and the O–C–O angle is widened [2,4–7]. All of these effects are measured relative to equatorial substitution, i.e., where no anti relationship of O-5 lone-pair density to the  $\sigma_{\text{C-1-O-1}}^*$  acceptor orbital exists.

The term ‘exo-anomeric effect’ [2] refers to a related structural feature, namely that the anomeric substituent generally prefers to be rotated so that the C-1–O-5 and O-1–R bonds are gauche. This results in O-1 lone-pair density being localized anti to the C-1–O-5 bond, and this effect on the O-5–C-1–O-1–R torsional coordinate is rationalized in an analogous manner to the anomeric effect [13].

Insofar as the geometrical consequences of the anomeric and exo-anomeric effects are opposed for the C-1–O-1 and C-1–O-5 bond lengths, it is possible for each of them to adopt a wide range of values. A survey of the Cambridge Crystal Structure Database shows, for example, that for a number of carbo-

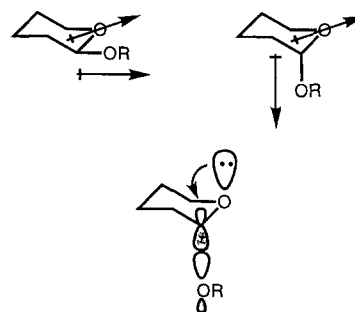
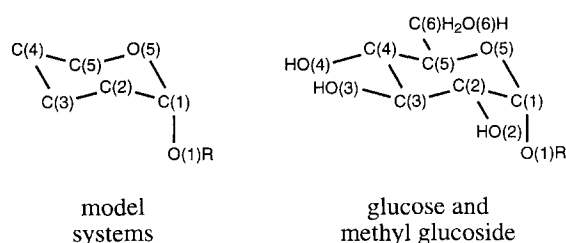


Fig. 1. Alignment of bond dipoles in the axial anomer of a 2-alkoxytetrahydropyran is more favorable than in the equatorial anomer. The dominant hyperconjugative interaction ascribed to the anomeric effect is also shown.

hydrates and carbohydrate-like molecules the C-1–O-1 bond is the shortest C–O bond, followed by the C-1–O-5 bond [37].

The purpose of this article is to employ theoretical methods, including the calculation of internal solute energies and free energies of aqueous solvation, to elucidate the energetic and geometric consequences of the anomeric and exo-anomeric effects. We focus upon the differences in several related model systems with axial disposition of the anomeric substituent (either hydroxy or methoxy) as illustrated in Fig. 2. Molecules **1–6** (where the subsequent **a** or **g** indicates an anti or gauche relationship, respectively, between the O-1–R bond and the C-1–O-5 bond) permit us to examine the effects of (i) anti versus gauche orientation of the O-1–R group, (ii) methoxy substitution at C-1 compared to hydroxy substitution, and (iii) a hydrogen bond acceptor or donor being present as a substituent at C-2. Natural Bond Orbital (NBO) analysis is applied to quantify individual contributions from different possible delocalizations to the energies of **a** and **g** conformers.

Because of the large number of potentially important conformers in carbohydrates, and because of the significant size of interesting polysaccharides, molecular mechanics methods have been, and will continue to be, used extensively to model these systems. The simplest molecular mechanics force fields, in particular those that fail to couple bond stretching, angle bending, and torsional motion, or that make torsional potentials dependent only on the two atoms of the rotating bond, cannot include hyperconjugation or other stereoelectronic effects. More complete force fields can include the energetic and geometrical consequences of the anomeric effect by addressing such deficiencies. For instance, the C–O–C–O torsional potential in the MM3 force field has been designed to



Scheme 1.

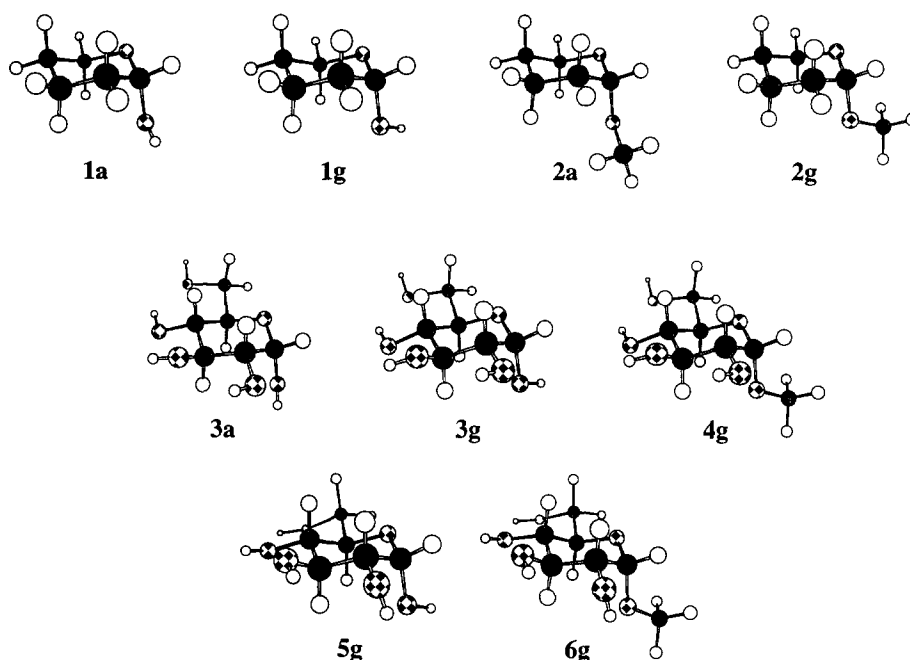


Fig. 2. Anti (a) and gauche (g) stereostructures calculated at the HF/cc-pVDZ level for 2-hydroxytetrahydropyran (1), 2-methoxytetrahydropyran (2),  $\alpha$ -D-glucose with a clockwise array of intramolecular hydrogen bonds (3), methyl  $\alpha$ -D-glucopyranoside with a clockwise array of intramolecular hydrogen bonds (4),  $\alpha$ -D-glucose with a counter-clockwise array of intramolecular hydrogen bonds (5), and methyl  $\alpha$ -D-glucopyranoside with a counter-clockwise array of intramolecular hydrogen bonds (6).

agree closely with high level ab initio calculations [23]. It continues, therefore, to be of great interest to compare quantum mechanical methods and molecular mechanics predictions for the anomeric and exo-anomeric effects as they affect molecular energies and geometries. The final section of this paper addresses precisely those issues.

## 2. Methods

All gas-phase quantum chemical calculations were carried out at the restricted Hartree–Fock (HF) level [38] employing the cc-pVDZ basis set [39]. We have previously observed that energies and geometries calculated at this level of theory are in good agreement with much more complete quantum mechanical calculations for glucose conformers [40,41]. With the exception of **2a**, all structures were fully optimized at this level of theory. Structure **2a** is not stationary; it was fully optimized subject to the constraint of the dihedral angle  $\omega[\text{R-O-1-C-1-O-5}]$  being held fixed at 178.9 deg (the value found at the HF/cc-pVDZ level for the corresponding dihedral angle in **1a**). If the constraint is relaxed, the structure converts smoothly to **2g**. Tvaroška and Carver similarly ob-

served this conformer to be non-stationary at the HF/6-31G\* level [21].

Hyperconjugative stabilization energies were calculated by second-order perturbation theory analysis of the off-diagonal Fock matrix elements in the natural bond orbital (NBO) basis [42]. In this method, hyperconjugation is measured in terms of bond-pair or lone-pair electron delocalization into an antibonding orbital (i.e.,  $\sigma \rightarrow \sigma^*$  or  $n \rightarrow \sigma^*$ ) and the energetic contribution of this delocalization relative to an idealized Lewis structure [42]. Because of the perturbative nature of this analysis, we believe that the absolute magnitudes of these energies are less meaningful than the relative magnitudes, and we will focus only on the latter. Similar uses of NBO analysis to examine hyperconjugative effects in various carbohydrate model systems have been reported by Petillo and Lerner [19] and Salzner and Schleyer [22].

Molecular mechanics calculations were carried out using the MM3(94) force field (the most recently available version) [43,44]. Electrostatic contributions to the force field energies were calculated from bond-dipole–bond-dipole interactions using a dielectric constant of 1.5 (the recommended value for gas-phase MM3 calculations [45–49]). With the exception of **2a**, all structures were fully optimized at

this level of theory. Structure **2a** is not stationary; it was fully optimized subject to the constraint of the dihedral angle  $\omega[\text{R}-\text{O}-1-\text{C}-1-\text{O}-5]$  being held fixed at  $147.9^\circ$  (the value found at the MM3(94) level for the corresponding dihedral angle in **1a**). If the constraint is relaxed, the structure converts smoothly to **2g**.

Solvation free energies were calculated with the aqueous Solvation Model 5.4/A [50] (SM5.4/A) making use of the Austin Model 1 [51] (AM1) semiempirical Hamiltonian, Class IV charges [52], and density descreening [50,53,54]. Solvation calculations employed frozen HF/cc-pVDZ geometries and permitted full relaxation of the solute electronic wave function in the presence of the aqueous medium. In this model, the standard state free energy of solvation is given by

$$\Delta G_S^\circ = \Delta G_{\text{ENP}} + G_{\text{CDS}} \quad (1)$$

where the standard state is taken as 1 M in both the gas phase and solution,  $\Delta G_{\text{ENP}}$  is the sum of the free energy gain due to electric polarization of the solvent and the associated electronic–nuclear energetic cost to the solute, and  $G_{\text{CDS}}$  accounts for first-hydration-shell effects.  $\Delta G_{\text{ENP}}$  was analyzed in terms of group contributions by dividing solvation effects on charge–charge interactions equally between the atoms involved according to a method (Method I [55]) previously described for partitioning solute reorganization energy; the atomic contributions are then summed over the group of interest.

Calculations were carried out with the GAUSS-94 program suite [56] (which incorporates NBO version 3.1 [57]), the MM3 program<sup>1</sup> [47] and a locally modified version of AMSOL version 5.2.1 [58].

### 3. Results and discussion

Compounds **1** and **2** are 2-hydroxy- and 2-methoxytetrahydropyran, respectively. (Although this nomenclature is correct for a substituted tetrahydropyran, we will continue below to use the atomic numbering scheme in Scheme 1 since it maintains consistency with accepted carbohydrate nomencla-

ture.) Such substituted tetrahydropyrans serve as simple model systems for investigating anomeric and exo-anomeric effects without complication from all of the other hydroxy and hydroxymethyl substituents present in glucose. Structures **1g** and **2g** have the preferred exo-anomeric orientation of the O-1-R group, while structures **1a** and **2a** do not.

Compounds **3** and **5** are  $\alpha$ -D-glucose conformers. By comparing calculations on these molecules to calculations on **1**, we can discern the consequences of having additional hydroxy groups on the tetrahydropyran ring. Of critical importance is the orientation of the O-2 hydroxy group. In **3**, it is rotated in such a manner that it can serve as a hydrogen-bond acceptor for O-1-H when O-1-H is appropriately rotated, as it is in **3a**. In **5**, on the other hand, the O-2H group can serve as a hydrogen-bond *donor* to O-1-H — in this instance, only conformer **5g** (which does have the O-2 to O-1 hydrogen bond) is considered because **5a** is not stationary at the ab initio level, presumably because of high steric repulsion energy.

Finally, compounds **4** and **6** are methyl  $\alpha$ -D-glucopyranoside conformers analogous to **3** and **5**, respectively. They are informative in comparison to **2** in the same manner that **3** and **5** may be compared to **1**. Moreover, **4** may be compared to **3** and **6** to **5** in order to ascertain the effects of methylation of O-1. For compound **4**, however, there is no stationary analogue to **3a** because the substitution of a  $\text{CH}_3$  group for an H at O-1 renders the anti conformer non-stationary at the ab initio level (and the same holds true for **6a**, although in this case the steric repulsion between the C-1 and C-2 substituents is a dominant factor).

The gas-phase results calculated at the HF/cc-pVDZ level are given in Tables 1 and 2 and are discussed in Section 3.1. SM5.4/A aqueous solvation free energies are given in Table 3 and are discussed in Section 3.2. Finally, selected aspects of the MM3(94) structural and energetic results are given in Table 4 and are discussed in Section 3.3.

*Gas-phase results.*—This section describes the gas-phase results with respect to geometries and energies; we focus on four specific comparisons of compounds. In the subsections below comparisons are made between **g** conformers and **a** conformers and between corresponding hydroxy- and methoxy-substituted conformers. An examination of the effect of an hydroxy group at C-2 when there is an hydroxy group at C-1 is made by comparing compounds **3** and **5** to **1**, and finally, an examination is made of the effect of an hydroxy group at C-2 when there is a

<sup>1</sup>The MM3 program is available to commercial users from Tripos Associates, 1699 South Hanley Rd., St. Louis, MO 63144, and to academic users from QCPE, Indiana University, Bloomington, IN 47405.

Table 1  
Selected geometric data for **1–6** at the HF/cc-pVDZ level <sup>a</sup>

Structure	R	$\omega_{\text{ROCO}}$ (deg)	$\angle_{\text{OCO}}$ (deg)	$r_{\text{C-1-O-1}}$ (Å)	$r_{\text{C-1-O-5}}$ (Å)	$r_{\text{C-1-C-2}}$ (Å)	$r_{\text{C-1-H}}$ (Å)
<b>1a</b>	H	178.9	107.8	1.400	1.381	1.527	1.092
<b>1g</b>	H	55.8	111.3	1.392	1.393	1.520	1.091
<b>2a</b>	CH <sub>3</sub>	178.9 <sup>b</sup>	107.3	1.400	1.382	1.529	1.093
<b>2g</b>	CH <sub>3</sub>	65.5	111.8	1.389	1.394	1.521	1.092
<b>3a</b>	H	195.1	109.3	1.388	1.385	1.525	1.090
<b>3g</b>	H	66.6	111.6	1.382	1.400	1.520	1.089
<b>4g</b>	CH <sub>3</sub>	72.9	111.8	1.377	1.400	1.520	1.090
<b>5g</b>	H	62.8	112.3	1.393	1.387	1.524	1.089
<b>6g</b>	CH <sub>3</sub>	67.7	112.6	1.388	1.388	1.525	1.091

<sup>a</sup> Structures were fully optimized unless otherwise indicated.

<sup>b</sup> The anti orientation of **2a** is not stationary, so  $\omega_{\text{ROCO}}$  was held fixed at the value optimized for **1a**.

methoxy group at C-1 by comparing compounds **4** and **6** to **2**.

*Rotation about the C-1–O-1 bond — comparison of a to g.* Compounds **1**, **2**, and **3** afford three opportunities to compare **a** conformers to **g** conformers. In the **g** conformers, there are several geometric features consistent with increased ‘classical’ exo-anomeric delocalization (i.e.,  $n_{\text{O-1}} \rightarrow \sigma_{\text{C(1)O(5)}}^*$  hyperconjugation) relative to the **a** conformers. In particular, Table 1 shows that the **g** conformers have O–C–O bond angles that are wider than those of the **a** conformers by 2.3 to 4.5. In addition, the C-1–O-1 bond lengths are shorter in the **g** conformers than in the **a** conformers by between 0.006 and 0.011 Å. Finally, the C-1–O-5 bond lengths are longer in the **g** conformers than in the **a** conformers by between 0.012 and 0.015 Å, respectively.

Focusing on a different part of the molecules, we note that the **g** conformers do not place O-1 lone-pair density anti to the C-1–C-2 bond, but the **a** conformers do. Consistent with increased hyperconjugative delocalization into  $\sigma_{\text{C(1)C(2)}}^*$  occurring for the latter structures, the C-1–C-2 bond is longer in the **a** conformers than in the **g** conformers by 0.005 to 0.008 Å.

Little variation is observed in the C-1–H bond length as a function of rotation about the C-1–O-1 bond. This observation is consistent with there being little difference in total hyperconjugative delocalization into  $\sigma_{\text{C(1)H}}^*$ , which might be expected insofar as there is an oxygen lone pair anti to this bond in either conformer.

Inspection of the NBO-derived delocalization energies is completely consistent with the conclusions reached above based on geometric analysis. The **g** conformers have  $n_{\text{O-1}} \rightarrow \sigma_{\text{CO}}^*$  delocalization energies that are 11.9 to 12.8 kcal/mol larger than those

calculated for **a**. Conversely, the **a** conformers have  $n_{\text{O-1}} \rightarrow \sigma_{\text{C(1)C(2)}}^*$  delocalization energies that are 6.7 to 8.5 kcal/mol larger than those calculated for **g**. The  $n_{\text{O-1}} \rightarrow \sigma_{\text{C(1)H}}^*$  delocalization energies are somewhat larger for the **a** conformers, 0.6 to 2.7 kcal/mol, but as noted above this difference does not manifest itself in any noteworthy effect on the C-1–H bond length. The net total  $n_{\text{O-1}} \rightarrow \sigma^*$  hyperconjugation into *all* relevant acceptor orbitals is larger for the **g** conformers by only 1.8 to 3.5 kcal/mol compared to the **a**. Thus, although  $n_{\text{O-1}} \rightarrow \sigma_{\text{C(1)O(5)}}^*$  delocalization is most effective for hyperconjugative stabilization, if it is reduced by conformational change then other delocalizations increase to offset some of the reduction.

We note that the net difference in hyperconjugative stabilization energies between **g** and **a** conformers does not account for the total energetic separation between these two conformers. Thus, and not unexpectedly, the full exo-anomeric effect must be regarded as a combination of steric, electrostatic, and hyperconjugative effects, a point which Tvaroška and Bleha have emphasized [5].

Comparison of **a** to **g** conformers is also of interest for understanding anomeric (as opposed to *exo*-anomeric) delocalization. Table 2 indicates that  $n_{\text{O-5}} \rightarrow \sigma_{\text{C(1)O(1)}}^*$  hyperconjugation is greater for the **g** conformers than the **a** by 0.6 and 1.1 kcal/mol for **1** and **2**, respectively. This effect probably arises in order to balance the charge shift associated with improved  $n_{\text{O-1}} \rightarrow \sigma_{\text{C(1)O(5)}}^*$  *exo*-anomeric stabilization already noted for these conformers and is accompanied by a slight decrease in  $n_{\text{O-5}} \rightarrow \sigma_{\text{C(1)C(2)}}^*$  delocalization. For structure **3**, however, the increase in anomeric stabilization for the **g** conformer is not observed. In addition, for structure **3** both the absolute magnitude of the  $n_{\text{O-1}} \rightarrow \sigma_{\text{C(1)O(5)}}^*$  *exo*-anomeric interaction energy in **3g** and the differential magni-

Table 2  
Absolute (au) and relative (kcal/mol) HF/cc-pVDZ energies and hyperconjugative stabilization energies (kcal/mol) from natural bond orbital analysis

Structure	HF energy <sup>a</sup>	exo-Anomeric effect				Anomeric effect			
		$n_{O(1)} \rightarrow \sigma_{CO}^*$	$n_{O(1)} \rightarrow \sigma_{CC}^*$	$n_{O(1)} \rightarrow \sigma_{CH}^*$	Total O-1	$n_{O(s)} \rightarrow \sigma_{CO}^*$	$n_{O(s)} \rightarrow \sigma_{CC}^*$	$n_{O(s)} \rightarrow \sigma_{CH}^*$	Total O-5
<b>1a</b>	–344.90654 (3.7) <sup>b</sup>	5.7	9.0	10.7	25.4	18.1	9.5	3.3	30.9
<b>1g</b>	–344.91237	17.6	1.2	10.1	28.9	18.7	9.1	3.0	30.8
<b>2a</b>	–383.92902 (4.7) <sup>c</sup>	6.9	9.8	10.5	28.2	17.6	9.3	3.2	30.1
<b>2g</b>	–383.93657	19.0	1.3	9.7	30.0	18.7	9.0	2.9	30.6
<b>3a</b>	–684.40760 (0.9) <sup>d</sup>	7.6	7.9	12.0	27.5	16.8	8.9	3.2	28.9
<b>3g</b>	–683.40476 (2.6) <sup>d</sup>	20.4	1.2	9.3	30.9	16.6	8.2	2.9	27.7
<b>4g</b>	–722.42912 (3.0) <sup>e</sup>	21.1	1.4	9.4	31.9	16.6	8.2	2.8	27.6
<b>5g</b>	–683.40898	18.3	1.1	9.0	28.4	19.5	9.3	3.1	31.9
<b>6g</b>	–722.43385	19.1	1.3	9.2	29.6	19.3	9.2	3.0	31.5

<sup>a</sup> Absolute energies are followed by relative energies in parentheses.

<sup>b</sup> Relative to **1g**.

<sup>c</sup> Relative to **2g**.

<sup>d</sup> Relative to **5g**.

<sup>e</sup> Relative to **6g**.

Table 3  
Aqueous solvation free energy components (kcal/mol) for **1–6**<sup>a</sup>

Structure	R	O-1 R group			O-5			Full solute		
		$\Delta G_{\text{ENP}}^b$	$G_{\text{CDS}}^o$	Group $\Delta G_s^o$	$\Delta G_{\text{ENP}}^b$	$G_{\text{CDS}}^o$	Atomic $\Delta G_s^o$	$\Delta G_{\text{ENP}}$	$G_{\text{CDS}}^o$	Total $\Delta G_s^o$
<b>1a</b>	H	−3.8	−0.2	−4.0	−2.4	−0.9	−3.3	−5.8	0.0	−5.8
<b>1g</b>	H	−2.9	0.1	−2.8	−1.5	−1.0	−2.5	−4.2	0.2	−4.1
<b>2a</b>	CH <sub>3</sub>	−2.3	0.4	−1.9	−2.3	−0.9	−3.2	−3.5	0.7	−2.9
<b>2g</b>	CH <sub>3</sub>	−1.7	0.6	−1.1	−2.1	−0.8	−2.9	−2.9	0.8	−2.1
<b>3a</b>	H	−2.5	−0.3	−2.8	−1.3	−0.5	−1.8	−9.6	−1.6	−11.1
<b>3g</b>	H	−3.5	0.6	−2.9	−0.4	−0.6	−1.0	−11.4	−0.9	−12.3
<b>4g</b>	CH <sub>3</sub>	−2.0	0.8	−1.2	−1.1	−0.4	−1.5	−9.3	−0.6	−9.9
<b>5g</b>	H	−1.7	0.6	−1.1	0.2	−0.5	−0.3	−8.8	−2.5	−11.4
<b>6g</b>	CH <sub>3</sub>	−0.2	0.8	0.6	−0.5	−0.4	−0.9	−6.9	−2.4	−9.3

<sup>a</sup> Calculated by SM5.4/A method at HF/cc-pVDZ geometries.

<sup>b</sup> Solute reorganization energy  $\Delta G_{\text{EN}}^b$  was assigned uniformly over all solute groups; see Methods section.

tude for this interaction (**3g** versus **3a**) are maximized compared to **1** and **2**. This can probably be ascribed to stronger lone-pair–lone-pair repulsions between O-1 and O-2 in the **g** conformer. In order to relieve this interaction in **3g**, delocalization of lone-pair density in an O-1 → O-5 sense is increased, and delocalization of lone-pair density in an O-5 → O-1 sense is reduced.

*Nature of the C-1 substituent — comparison of methoxy to hydroxy.* Methylation of the C-1 hydroxy group leads to a significant change in the R–O–C–O dihedral angle in each pair of corresponding **g** conformers (**1g** versus **2g**, **3g** versus **4g**, and **5g** versus **6g**). In particular, this angle is 4.9° to 10.7° larger in each pyranoside than in the corresponding pyranose. This probably results from an attractive electrostatic interaction between the proton on O-1 and lone-pair

density on O-5 in the pyranose compounds that is not available to the pyranosides. No comparison of this dihedral angle for the **a** conformers is possible, since no stationary **a** pyranosides were found. While steric repulsion would be severe for **a** conformers of structures **4** and **6**, it is less obvious that **2a** should be non-stationary. With the R–O–C–O dihedral angle in **2a** constrained to the same value optimized for **1a**, the difference in energy between **2g** and **2a** (4.7 kcal/mol favoring **2g**) is only 1 kcal/mol larger than the difference calculated for **1g** and **1a**. This suggests that the rotational potential about the C-1–O-1 bond is relatively flat near the anti orientation, and weak interactions give rise to a shallow minimum for **1a** but not for **2a**. Tvaroška and Carver mapped out the C-1–O-1 rotational potential for **2** at a variety of ab initio levels, and indeed found it to be very flat in the

Table 4  
Selected geometric data and relative energies for **1–6** at the MM3(94) level<sup>a</sup>

Structure	R	Rel <i>E</i> (kcal/mol)	$\omega_{\text{ROCO}}$ (deg)	$\angle_{\text{OCO}}$ (deg)	$r_{\text{C-1-O-1}}$ (Å)	$r_{\text{C-1-O-5}}$ (Å)	$r_{\text{C-1-C-2}}$ (Å)	$r_{\text{C-1-H}}$ (Å)
<b>1a</b>	H	1.7 <sup>b</sup>	147.9	107.5	1.437	1.413	1.526	1.116
<b>1g</b>	H	0.0	52.0	108.6	1.430	1.417	1.526	1.119
<b>2a</b>	CH <sub>3</sub>	3.1 <sup>c</sup>	147.9 <sup>d</sup>	106.5	1.426	1.413	1.527	1.117
<b>2g</b>	CH <sub>3</sub>	0.0	74.5	109.6	1.418	1.422	1.528	1.117
<b>3a</b>	H	−0.6 <sup>c</sup>	190.9	107.2	1.435	1.409	1.523	1.116
<b>3g</b>	H	1.6 <sup>c</sup>	65.2	107.0	1.429	1.421	1.523	1.116
<b>4g</b>	CH <sub>3</sub>	0.6 <sup>f</sup>	77.1	108.0	1.418	1.423	1.525	1.115
<b>5g</b>	H	0.0	51.9	108.4	1.431	1.418	1.525	1.117
<b>6g</b>	CH <sub>3</sub>	0.0	74.5	109.4	1.418	1.423	1.527	1.115

<sup>a</sup> Structures were fully optimized except for **2a**.

<sup>b</sup> Relative to **1g**.

<sup>c</sup> Relative to **2g**.

<sup>d</sup> The anti orientation of **2a** is not stationary, so  $\omega_{\text{ROCO}}$  was held fixed at the value optimized for **1a**.

<sup>e</sup> Relative to **5g**.

<sup>f</sup> Relative to **6g**.

region of **2a**, but they did not consider the same rotation for **1** [21].

Slight shortenings of the C-1–O-1 bonds (less than 0.006 Å) are also observed upon methylation. Shortening of the C-1–O-1 bond upon methylation is contrary to what might be expected on steric grounds; this phenomenon is therefore attributed to the methoxy group's being a slightly better donor in a hyperconjugative sense than hydroxy. Table 2 bears this out in that  $n_{O-1} \rightarrow \sigma_{C(1)O(5)}^*$  interaction energies increase by 0.7 to 1.4 kcal/mol upon methylation of O-1. In contrast, no significant trends in O-5 delocalization energies are noted upon methylation.

*Influence of a C-2 hydroxy group on pyranoses.* We begin with a comparison of **1** and **3**. The most significant difference between these structures as far as the anomeric and exo-anomeric effects are concerned is the presence in **3** of a hydroxy group at C-2 that can serve as a hydrogen bond acceptor when the O-1–H hydroxy group is in the **a** conformation. The H-bond length is 2.225 Å with an O-1–H–O-2 angle of 111.2°. In order to maximize this interaction, the H–O–C–O dihedral angle increases by 16.2 in **3a** compared to **1a**, and, very significantly, it overcomes the exo-anomeric preference for **g** over **a** for the O-1–H orientation. We can estimate the energy associated with this hydrogen bond by comparing the differences in energies between the **g** and **a** conformers for **1** and **3**. As noted above, **1a** is higher in energy than **1g** by 3.7 kcal/mol; conversely, **3a** is lower in energy than **3g** by 1.8 kcal/mol. This suggests that the OH-1–O-2 hydrogen bond energy in **3a** is worth about 5 to 6 kcal/mol.

The presence of the hydroxy group at C-2 in a hydrogen-bond-acceptor orientation has significant effects on the hyperconjugative stabilizations as well. In particular, in both the **g** and the **a** conformations, exo-anomeric  $n_{O-1} \rightarrow \sigma_{C(1)O(5)}^*$  interactions are larger for **3** than for **1**, and the anomeric  $n_{O-5} \rightarrow \sigma_{C(1)O(1)}^*$  interactions are correspondingly smaller. For the **g** conformation, this has been discussed in the foregoing section as deriving from the repulsion between lone pairs on O-1 and O-2. For the **a** conformer the explanation is similar insofar as the O-1–H–O-2 hydrogen bond makes the donor oxygen, O-1, more negative, and this extra electron density can be delocalized by increased activity as a hyperconjugative donor and decreased activity as an acceptor.

For the **g** orientation, we may additionally compare the effects of having the hydroxy group at C-2 oriented to serve as a hydrogen bond donor, as in **5g**. As in the acceptor orientation, interactions with the

C-2 hydroxy have significant effects on the H–O-1–C-1–O-5 dihedral angle. In **3g**, where the effect is O-1–O-2 lone-pair–lone-pair repulsion, the angle is 10.8° larger than in **1g**. In **5g**, where the effect is formation of an H-2–O-1 hydrogen bond, the angle is 7.0° larger than in **1g**.

An additional effect of hydrogen bond donation to O-1 is to render the O-1–H hydroxy group a better hyperconjugative acceptor and a worse donor. One geometric consequence of this is the significant shortening of the C-1–O-5 bond in **5g** compared to **1g**. NBO analysis indicates that, relative to **1g**, in **5g** the  $n_{O-5} \rightarrow \sigma_{C(1)O(1)}^*$  interaction energy increases by 0.8 kcal/mol, and the sum of all  $n_{O-1} \rightarrow \sigma^*$  interaction energies decreases by 0.5 kcal/mol.

*Influence of a C-2 hydroxy group on methylpyranosides.* In the pyranosides, comparisons of features in systems with and without a C-2 hydroxy group are restricted to **g** conformers, since, as discussed above, we did not find stationary structures corresponding to **4a** and **6a**. Within the **g** series, trends among **2**, **4**, and **6** are similar to those observed for **1**, **3**, and **5**. In particular, repulsive interactions between adjacent oxygen lone pairs on O-1 and O-2 in **4g** lead to an increase in O-1 hyperconjugative donor interactions and a decrease in O-1 hyperconjugative acceptor interactions relative to **2g**; in magnitude these changes are about 2 kcal/mol. This effect causes **4g** to have the largest hyperconjugative stabilization energy among **1–6** for O-1 acting as donor and the smallest hyperconjugative stabilization energy among **1–6** for O-1 acting as acceptor. This situation is further reflected in a 0.012 Å shorter C-1–O-1 bond length and a 0.006 Å longer C-1–O-5 bond length for **4g** than is found for **2g**. These bond lengths in **4g** represent the minimum and maximum values, respectively, observed in **1–6**.

The effect of hydrogen bond-donation to O-1, as gauged by comparison of **2g** and **6g**, is quite similar to the situation observed for **1g** and **5g**. Here, hydrogen bonding stabilizes negative charge localization at O-1, and as a result the  $n_{O-5} \rightarrow \sigma_{C(1)O(1)}^*$  anomeric delocalization increases by 0.6 kcal/mol while the total  $n_{O-1} \rightarrow \sigma^*$  exo-anomeric delocalization decreases by 0.4 kcal/mol. A geometric feature associated with this alteration in the electronic structure is the 0.006 Å shortening of the C-1–O-5 bond.

*Effects of aqueous solvation.*—In this section we consider differences in solvation free energies as a function of conformation and other factors. As indicated in Eq. (1), these solvation free energies have two components [50,59,60]. The first,  $\Delta G_{\text{ENP}}$ , is asso-



ciated with the favorable mutual polarization energies of the solute and solvent, where the solvent is approximated as a dielectric continuum. The second,  $G_{\text{CDS}}$ , measures effects associated with the first solvation shell, e.g., cavitation, dispersion, solvent structural rearrangements, and electrostatic deviations from bulk behavior.

$\Delta G_{\text{ENP}}$  is calculated using atomic partial charges [50,59], in particular, from atomic charges calculated self consistently in solution [55,59,61], since relaxation of the electronic structure in response to solvation can change the atomic partial charges. In all of the cases considered here, we found that the largest change in any atomic partial charge upon solvation is 0.03 units, which indicates that these molecules are not especially polarizable. Thus, the extent to which different conformers are solvated differently is driven primarily by differences in the gas-phase electronic distribution and not by significantly different degrees of solvent-induced electronic polarization. This general result is in contrast to the much larger calculated effects of solvation on charge distributions in model anomeric systems bearing a formal charge [17].

Focusing for the moment on the dipole–dipole component of the exo-anomeric effect, it is evident that solvation should decrease the magnitude of this interaction, that is, the solvent dielectric will screen the interaction between the O-1–H dipole and the C-1–O-5 dipole. This screening reduces the difference between the energies of **a** conformers, where the two bond dipoles are aligned, and **g** conformers, where the two are approximately antiparallel. However, this dipole–dipole interaction is but one of many in the glucose and glucoside systems, so it may be that the effect of solvation on interactions other than the exo-anomeric one plays a larger role in dictating conformational preference for these molecules. This is seen to be the case for **3**, as discussed further below.

The remainder of this section is subdivided identically to the previous section in order to highlight the effects of solvation on those differences previously discussed for the gas phase.

*Rotation about the C-1–O-1 bond — comparison of **a** to **g**.* In the simple model systems **1** and **2**, the **a** conformer is better solvated than the **g** conformer by 1.7 kcal/mol in the hydroxy case and by 0.8 kcal/mol in the methoxy case. Table 3 shows that this results almost completely from changes in the solvation of the O-1–R group and the tetrahydropyran ring oxygen O-5. Both groups become less well solvated in the **g** conformer. This results from a

combination of several factors. First, because of improved hyperconjugative delocalization, the charge on O-1 in the **g** conformer is 0.02 units less negative than in the **a** conformer — this reduces  $\Delta G_{\text{ENP}}$  for the O-1–R group. Although there is a corresponding *increase* in negative charge at O-5 for these conformers, this does not lead to a net increase in solvation free energy at that position for either **1** or **2**. In **1**, rotation of the hydroxy group brings the positively charged proton into the same region of space as the negatively charged tetrahydropyran oxygen. The solvent cannot optimally solvate both charges simultaneously, and as a result the favorable electrostatic solvation of both charges is decreased in magnitude. In **2**, on the other hand, the bulky methoxy group descreens O-5 when it is in the **g** conformation (i.e., it replaces solvent and thereby decreases favorable polarization interactions associated with solvent screening of internal solute electrostatics). In the **a** conformation, the concentration of lone-pair density from both the O-1 and O-5 oxygen atoms into the same region of space leads to an especially favorable polarization interaction, and that too is reflected in the overall increase in  $\Delta G_{\text{ENP}}$  for the O-1–R and O-5 groups in **1a** and **2a**. The CDS terms, on the other hand, are not very sensitive to conformation in **1** and **2**.

Our results for the relative solvation free energies of **2a** and **2g** may be compared to the results of Jorgensen et al. [34], who used the OPLS/AMBER molecular mechanics force field [34,62] for the solute and the TIP4P [63] explicit water model to study this system, and also to the results of Tvaroška et al. [21,24], who used a (nonpolarizable) continuum model with corrections for nonelectrostatic effects [24,64] for this same purpose. Tvaroška and Kožar calculated **2g** to be better solvated than **2a** by 0.8 kcal/mol using molecular dipole and quadrupole moments calculated at a semiempirical level [24]; our calculations predict exactly the same preference for **2g**. The quantitative agreement between the two quite different methods for accounting for solvation increases confidence in the physicality of the results.

A later calculation by Tvaroška and Carver using molecular dipole and quadrupole moments calculated at the HF/6-31G\* level found **2g** to be better solvated than **2a** by 1.7 kcal/mol [21]. This level of ab initio theory, however, is well known to overestimate molecular dipole moments [38], and this may account for the calculated increase in differential solvation. Jorgensen et al. found **2g** to be better solvated than **2a** by 1.8 kcal/mol [34]. However, their calculations

also overestimate the differential free energy of solvation between **2g** and the lowest energy equatorially substituted conformer, i.e., the solvation effect on the anomeric effect, by about 1 kcal/mol (based on comparison to experiment for related systems [21,33]). The calculations of Tvaroška and Kožar [24], as well as our own [65], are consistent with experimental measurements of the effect of aqueous solvation on the anomeric effect [21], suggesting that they are overall more reliable.

The situation is considerably more complex for comparing **3a** to **3g** because so many interacting groups are present in glucose. In this instance, in contrast to the results for **1** and **2**, the overall  $\Delta G_{\text{ENP}}$  is larger for **3g** than **3a**. This can be understood from examination of the contribution of different functional groups in glucose to the overall solvation free energy. The reduced magnitude of  $\Delta G_{\text{ENP}}$  in **3a** compared to **3g** is associated with the presence of the O-1–H–O-2 intramolecular hydrogen bond in **3a**. While this is a favorable interaction in a gas-phase sense, it reduces the exposure of O-2 lone-pair density and the O-1 hydroxy proton to solvent. Moreover, the concentration of O-1 and O-2 lone-pair density into the same region of space in the **g** conformer is an especially favorable situation for solvation. The combination of these effects is part of the 1.2 kcal/mol decrease in solvation free energy calculated for **3a** relative to **3g**. Interestingly, examination of group contributions indicates that most of this effect is partitioned into changes in solvation of the O-2 and O-5 groups — the differential solvation effect on O-1–H is very small. Again, this reflects a delicate balance. Although the O-1–H group is better exposed to solvent in the **g** conformation, this places the positive proton near to the negative O-5 lone-pair density (vide supra); this decreases the magnitude of the negative  $\Delta G_{\text{ENP}}$  contribution of both the O-5 atom and the O-1–H group to the overall solvation free energy. This comparison provides a good example of the leveling effect of solvation on hydroxy conformations in sugar molecules and simple analogues, which we have also discussed elsewhere [30,40,66]; i.e., whenever a conformational potential energy surface is dominated by intramolecular electrostatic interactions, solvent will partially level it (when steric effects dominate, on the other hand, solvation effects can move relative energies in either direction). Note that when the solvation free energy is added to the HF/cc-pVDZ gas-phase energy, **3a** is found to be only 0.6 kcal/mol lower than **3g**.

*Nature of the C-1 substituent — comparison of*

*methoxy to hydroxy*. In every case, methylation decreases the magnitude of the negative solvation free energies of the pyranosides relative to the pyranoses by 2.0 to 2.9 kcal/mol. This reflects the hydrophobicity of a methyl group compared to a hydroxy proton.

Interestingly, methylation in the **g** conformers makes  $\Delta G_{\text{ENP}}$  for O-5 more negative by 0.6 to 0.7 kcal/mol. This seems counterintuitive at first glance, because the methyl group is larger than H, and thus must have a larger descreening effect on O-5. However, replacing the small *positively* charged hydroxy proton at that position in space with a charge-neutral methyl group allows organization of the solvent to solvate optimally the *negative* charge at O-5. The descreening effect is, however, clearly seen in the changes calculated for first-solvation-shell effects upon methylation of the **g** conformers;  $G_{\text{CDS}}$  for O-5 becomes less negative by 0.1 to 0.2 kcal/mol because of decreased exposure.

*Influence of a C-2 hydroxy group on pyranoses*. By comparison of group contributions to the solvation free energies of **1g** and **3g**, we see that the effect of the C-2 hydroxy on the solvation free energy of the O-1–H group in **3g** is negligible. In **5g**, on the other hand, the donation of a hydrogen bond to O-1 coincides with a decrease in the magnitude of the negative solvation free energy for this group by 1.7 kcal/mol. As discussed above for **3g** versus **3a**, we infer that the favorable gas-phase interaction of an intramolecular hydrogen bond decreases the solvation free energy associated with the interacting groups. This can also be seen by comparing the total free energies of solvation for **3a**, **3g**, and **5g**. There are four intramolecular hydrogen bonds in both **3a** and **5g**, but only three in **3g**; correspondingly, **3g** is about a kcal better solvated than **3a** and **5g**.

The solvation free energies associated with O-5 in **3a**, **3g**, and **5a** are significantly smaller than in the analogous conformers **1a** and **1g**. This is not an effect associated with the C-2 hydroxy group, but rather with the presence of the exocyclic hydroxymethyl group in the glucose structures. This bulky group descreens O-5, and this contributes to the solvation free energy of O-5 being less negative by 1.5 kcal/mol in both conformers of **3** compared to **1**. Interestingly, the O-5 group makes a 0.7 kcal/mol less negative contribution to  $\Delta G_{\text{s}}^{\circ}$  in **5g** compared to **3g**, and this difference results almost entirely from  $\Delta G_{\text{ENP}}$ . After careful consideration of the solvation free energies for all of the groups and their interactions, it is not clear that this decrease can be assigned

to any specific structural or electronic effect. Rather, it serves as a good illustration of how significant amounts of solvation free energy can be tied up in very complex interactions involving several centers carrying significant partial charges.

Another example of the complexity of these interactions is that even though the group contributions associated with O-1-H and O-5 make the solvation of **3g** 2.5 kcal/mol more negative (more favorable) than the solvation of **5g**, the net difference over the entire solute is only 0.9 kcal/mol. Changes associated primarily with the other hydroxy groups somewhat offset the effects at the anomeric oxygens.

*Influence of a C-2 hydroxy group on methylpyranosides.* Table 3 shows that there are no real changes in the effects just discussed for the pyranoses when O-1 is methylated. The intramolecular hydrogen bond in **6g** makes this conformer less well solvated than **4g**, where it does not occur, by 0.6 kcal/mol. Again, this net result derives from a combination of large effects at O-1-R and O-5 that are partially offset by interactions associated primarily with the other hydroxy groups.

*Molecular mechanics calculations.*—Based on our experience with more complete levels of theory for both energies and structures of glucose [40,41], we consider the HF/cc-pVDZ results to be good benchmarks. For example, with respect to HF/cc-pVDZ energies, we have found that the relative energies of **3a**, **3g**, and **5g** change by no more than 0.15 kcal/mol when basis set and electron correlation effects are taken into account at a much higher level (this level is described elsewhere [40]). With respect to structures, we find HF/cc-pVDZ structures to be in very good agreement with MP2/cc-pVDZ structures (where MP2 denotes second-order Møller-Plesset perturbation theory [38]), and the latter have been found to compare favorably with single-crystal X-ray structures [40,41]. In this light, comparison of Table 4 to Table 1 and the relative energies in Table 2 should provide a good test of the MM3(94) force field.

We begin by comparing the MM3(94) relative energies to those calculated at the HF/cc-pVDZ level. In structures **1** and **2**, the anti conformers are less stable than the gauche by 3.7 and 4.7 kcal/mol, respectively, at the ab initio level. However, these differences are reduced to 1.7 and 3.1 kcal/mol, respectively, at the MM3(94) level; this difference indicates that the MM3(94) calculations do not adequately account for the exo-anomeric effect. It should be noted that in the case of **2**, these results would

probably be somewhat improved by forcing both the ab initio and the MM3(94) **2a** conformers to have the same O-C-O-C torsion angle [21].

In addition, of the three glucose conformers considered, MM3(94) predicts **3a** to be the one with the lowest energy, by 0.6 kcal/mol. This disagrees with the HF/cc-pVDZ results, which place **5g** lower than **3a** by 0.9 kcal/mol. Thus, in every case, anti conformers are found to be less destabilized relative to gauche at the MM3(94) level of theory by about 1 to 2 kcal/mol compared to HF/cc-pVDZ. Finally, the MM3(94) calculations also appear to underestimate the energy of **3g** relative to **5g** — in this case the disparity compared to the HF/cc-pVDZ level is 1.0 kcal/mol. While the **1a/1g**, **2a/2g**, and **3a/5g** errors are measures of the inability of MM3(94) to model adequately the exo-anomeric effect, the **3g/5g** difference is a measure of its inability to assess quantitatively the importance of the O-2-O-1 hydrogen bond in **5g**, in particular, this hydrogen-bond strength appears to be overestimated, perhaps because of its failure to account for exo-anomeric delocalization of O-1 lone-pair density.

Next we consider the accuracy of MM3(94) geometries. The MM3(94) results agree with the ab initio ones that structure **2a** is not stationary with respect to internal rotation about the C-1-O-1 bond. For the eight stationary structures in the tables, the force field predictions for the dihedral angles  $\omega$ [R-O-1-C-1-O-5] are in reasonable accord with the ab initio results. In particular, the average unsigned difference between the two levels of theory is 9°. However, this average difference is dominated by the difference for **1a**, which is 31°. When **1a** is removed from the averaging the average difference drops to 5.8°.

MM3(94) appears to underestimate consistently the O-5-C-1-O-1 valence angle. Averaged over all structures, the MM3(94) O-5-C-1-O-1 valence angles are 2.6 smaller than those calculated at the HF/cc-pVDZ level. Moreover, the increase in the O-5-C-1-O-1 valence angle upon going from an anti conformer to a gauche conformer (i.e., associated with the exo-anomeric effect) is smaller at the MM3(94) level than at the HF/cc-pVDZ level. As discussed in the previous section, this angle widening is a classic signature of the exo-anomeric effect, so this shortcoming of MM3(94) is consistent with the above conclusion that it does not adequately account for the exo-anomeric effect. Thus, in **1g** the O-5-C-1-O-1 valence angle is 1.1 larger than in **1a** at the MM3(94) level; the difference is 3.5 at the HF/cc-

pVDZ level. In **3g** the O-5–C-1–O-1 valence angle is actually 0.2 *smaller* than in **3a** at the MM3(94) level; the difference is 2.3 in the opposite direction (i.e., larger angle for **3g**) at the HF/cc-pVDZ level.

Finally, we compare the bond length data in Table 4 to that in Table 1. The bond lengths reported in Table 4 are taken directly from the force-field calculations, which were designed to reproduce experimental  $r_g$  bond lengths from electron diffraction measurements. Thus, we interpret these as predictions of  $r_g$  values and we can convert them to predictions of  $r_e$  values, which represent the minimum on the bond stretch potential energy curve, by using information about the bond stretch anharmonicity. In **1–6**, this tends to shorten all of the heavy-atom–heavy-atom bonds by about 0.01 Å and all of the C–H bonds by about 0.024 Å. With this in mind, it is apparent that all of the calculated C-1–O-1 and C-1–O-5 bond lengths are 0.02 to 0.03 Å longer at the MM3(94) level than at the HF/cc-pVDZ level. This is in very good agreement with bond lengths calculated at the MP2/cc-pVDZ level [67], i.e., these bond lengths are underestimated at the HF/cc-pVDZ level. The C-1–C-2 bonds, on the other hand, are up to 0.01 Å *shorter* at the MM3(94) level compared to the HF/cc-pVDZ level. Since the HF/cc-pVDZ C-1–C-2 bond lengths are themselves shorter than those calculated at the MP2/cc-pVDZ level by a few thousandths of an angstrom [67], it appears that the force field fails to account for anomeric lengthening of this bond, even though it performs reasonably for the C-1–O-1 and C-1–O-5 bonds.

More importantly, the force field has difficulty reproducing changes in bond lengths as a function of the exo-anomeric effect, again consistent with its inability to account for stereoelectronic effects. For instance, at the HF/cc-pVDZ level, when conformer **1a** is converted to **1g**, the C-1–O-1 bond shortens by 0.008 Å, the C-1–O-5 bond lengthens by 0.012 Å, and the C-1–C-2 bond shortens by 0.007 Å. At the MM3(94) level, the shortening of the C-1–O-1 bond is well reproduced (0.007 Å), but the lengthening of the C-1–O-5 bond is significantly underestimated (0.004 Å) and no change at all is predicted for the C-1–C-2 bond. For **2g/2a** and **3g/3a**, MM3(94) also fails to predict the shortening of the C-1–C-2 bond in the **g** conformers from decreased hyperconjugation into  $\sigma_{C(1)C(2)}^*$  (vide supra). In addition, for **2g/2a** and **3g/3a**, MM3(94) underestimates the changes in C-1–O-1 and C-1–O-5 bond lengths by comparison to HF/cc-pVDZ, but only by an average of about 0.002 Å. So, the geometric consequences of

the anomeric and exo-anomeric effects for the C-1–O-1 and C-1–O-5 bond lengths seem to be handled reasonably well by the force field, but effects on the C-1–C-2 bond length and the O-5–C-1–O-1 valence angle are handled less well, and as noted above, the energetic consequences are also not well predicted.

The MM3(94) component of this study makes it clear that the anomeric center poses a significant challenge for modeling with molecular-mechanics-based methods. In particular, taking the criteria for adequate performance of a computational model to be accurate prediction of relative energies to within 1 kcal/mol, bond lengths to within 0.01 Å, valence angles to within 1°, and torsion angles to within 5°, we note that the values calculated with the MM3(94) force field differ from the HF/cc-pVDZ values by larger margins, and our experience shows the latter to be more accurate in comparison to selected crystal structures. We conclude that additional atom types and/or specific stretch-torsion terms are required in order to predict more accurately carbohydrate structures and energies by such methods. We note with interest that the torsional potential about anomeric linkages in the GROMOS force field [68] for carbohydrates has very recently been modified in just such a way [69] in order to account more accurately for the energetics of this process, but the structural consequences of this modification remain to be reported.

#### 4. Conclusions

In 2-hydroxytetrahydropyran, hyperconjugative delocalization of O-1 lone-pair density into  $\sigma_{C(1)O(5)}^*$  is maximized for the gauche orientation of the O-5–C-1–O-1–R relative to anti. This exo-anomeric effect lengthens the C-1–O-5 bond, shortens the C-1–O-1 bond, and stabilizes the gauche conformers of **1** and **2** by about 4 kcal/mol over the anti. In the anti orientation, hyperconjugative interaction increases into other appropriately oriented  $\sigma^*$  orbitals, but the geometric and energetic consequences are less marked. In glucose, interactions of an O-1 hydroxy proton or of O-1 lone-pair density with a hydroxy group at C-2 acting as either a donor or acceptor can significantly affect these interactions. Trends observed in both pyranose systems are largely maintained in the corresponding pyranoside systems, although the anti conformer is no longer stationary even in 2-methoxytetrahydropyran **2**.

As expected on the basis of solute charge distributions, solvation effects oppose the exo-anomeric ef-

fect in **1** and **2**. More detailed analysis shows that this derives not only from changes in the charge distribution but also from decreased accessibility of the hydrophilic groups in the gauche conformers. Methylation of O-1 decreases the overall solvation free energy for all of the studied systems by about 2 kcal/mol. In the glucose and glucoside systems, the presence of additional functionality complicates the solvation, although certain trends are evident, e.g., solvation effects oppose the formation of intramolecular hydrogen bonds.

Finally, we examined the ability of MM3(94) force field calculations to account for energetic and geometrical differences in these related systems. We found systematic errors in energies, bond angles, and selected bond distances that can all be traced to an underestimation of the exo-anomeric effect by the force field. Evidently further force field refinements are necessary to address this challenge.

### Acknowledgements

We thank Lou Allinger, Carl Ewig, and Peter Petillo for illuminating discussions on the subject of the anomeric effect. This work was supported by the National Science Foundation.

### References

- [1] C.L. Jungius, *Z. Phys. Chem.*, **52** (1905) 97–108.
- [2] R.U. Lemieux, in P. de Mayo (Ed.), *Molecular Rearrangements*, Interscience, New York, 1964, pp 709–769.
- [3] C.G. Pearson and O. Rumquist, *J. Org. Chem.*, **33** (1968) 2572–2574.
- [4] A.J. Kirby, *The Anomeric Effect and Related Stereoelectronic Effects at Oxygen*, Springer-Verlag, Berlin, 1983.
- [5] I. Tvaroška and T. Bleha, *Adv. Carbohydr. Chem. Biochem.*, **47** (1989) 45–123.
- [6] G.R.J. Thatcher (Ed.), *The Anomeric Effect and Associated Stereoelectronic Effects*, ACS Symposium Series 539, American Chemical Society, Washington, DC, 1993.
- [7] P.P. Graczyk and M. Mikolajczyk, in E.L. Eliel and S.H. Wilen (Eds.), *Topics in Stereochemistry*, Vol. 21, John Wiley & Sons, New York, 1994, pp 159–349.
- [8] J.T. Edward, *Chem. Ind. (London)*, (1955) 1102–1104.
- [9] C.B. Anderson and D.T. Sepp, *Tetrahedron*, **24** (1968) 1707–1715.
- [10] V.G.S. Box, *Heterocycles*, **31** (1990) 1157–1181.
- [11] C. Romers, C. Altona, H.R. Buys, and E. Havinga, *Top. Stereochem.*, **4** (1969) 39–97.
- [12] G.A. Jeffrey, J.A. Pople, and L. Radom, *Carbohydr. Res.*, **25** (1972) 117–131.
- [13] S. Wolfe, M.-H. Whangbo, and D.J. Mitchell, *Carbohydr. Res.*, **69** (1979) 1–26.
- [14] G.A. Jeffrey and J.H. Yates, *Carbohydr. Res.*, **96** (1981) 205–213.
- [15] K.B. Wiberg and M.A. Murcko, *J. Am. Chem. Soc.*, **111** (1989) 4821–4828.
- [16] M.C. Krol, C.J.M. Huige, and C. Altona, *J. Comp. Chem.*, **11** (1990) 765–790.
- [17] C.J. Cramer, *J. Org. Chem.*, **57** (1992) 7034–7043.
- [18] E. Juaristi and G. Cuevas, *Tetrahedron*, **48** (1992) 5019–5087.
- [19] P.A. Petillo and L.E. Lerner, in G.R.J. Thatcher (Ed.), *The Anomeric Effect and Related Stereoelectronic Effects*, ACS Symposium Series 539, American Chemical Society, Washington, DC, 1993, pp 156–175.
- [20] U. Salzner and P.V.R. Schleyer, *J. Am. Chem. Soc.*, **115** (1993) 10231–10236.
- [21] I. Tvaroška and J.P. Carver, *J. Phys. Chem.*, **98** (1994) 9477–9485.
- [22] U. Salzner and P.v.R. Schleyer, *J. Org. Chem.*, **59** (1994) 2138–2155.
- [23] J.R. Kneisler and N.L. Allinger, *J. Comp. Chem.*, **17** (1996) 757–766.
- [24] I. Tvaroška and T. Kožár, *J. Am. Chem. Soc.*, **102** (1980) 6929–6936.
- [25] I. Tvaroška and T. Kožár, *Int. J. Quant. Chem.*, **23** (1983) 765–778.
- [26] J.-P. Praly and R.U. Lemieux, *Can. J. Chem.*, **65** (1987) 213–223.
- [27] R. Montagnani and J. Tomasi, *Int. J. Quant. Chem.*, **39** (1991) 851–870.
- [28] S. Ha, J. Gao, B. Tidor, J.W. Brady, and M. Karplus, *J. Am. Chem. Soc.*, **113** (1991) 1553–1557.
- [29] O. Kysel and P. Mach, *J. Mol. Struct. (Theochem)*, **227** (1991) 285–293.
- [30] C.J. Cramer and D.G. Truhlar, *J. Am. Chem. Soc.*, **115** (1993) 5745–5753.
- [31] B.P. van Eijck, R.W.W. Hooft, and J. Kroon, *J. Phys. Chem.*, **97** (1993) 12093–12099.
- [32] C.L. Perrin and K.B. Armstrong, *J. Am. Chem. Soc.*, **115** (1993) 6825–6834.
- [33] K.B. Wiberg and M. Marquez, *J. Am. Chem. Soc.*, **116** (1994) 2197–2198.
- [34] W.L. Jorgensen, P.I.M. Detirado, and D.L. Severance, *J. Am. Chem. Soc.*, **116** (1994) 2199–2200.
- [35] C.L. Perrin, K.B. Armstrong, and M.A. Fabian, *J. Am. Chem. Soc.*, **116** (1994) 715–722.
- [36] E.S. Marcos, R.R. Pappalardo, J.L. Chiara, M.C. Domene, J.M. Martínez, and R.M. Parrondo, *J. Mol. Struct. (Theochem)*, in press.
- [37] L. Schliefer, H. Senderowitz, P. Aped, E. Tartakovsky, and B. Fuchs, *Carbohydr. Res.*, **206** (1990) 21–39.
- [38] W.J. Hehre, L. Radom, P.v.R. Schleyer, and J.A. Pople, *Ab Initio Molecular Orbital Theory*, Wiley, New York, 1986.

- [39] T.H. Dunning, *J. Chem. Phys.*, 90 (1989) 1007–1023.
- [40] S.E. Barrows, F.J. Dulles, C.J. Cramer, D.G. Truhlar, and A.D. French, *Carbohydr. Res.*, 276 (1995) 219–251.
- [41] S.E. Barrows, J.W. Storer, C.J. Cramer, D.G. Truhlar, G. Johnson, and A.D. French, to be published.
- [42] A.E. Reed, F. Weinhold, L.A. Curtiss, and D.J. Pochatko, *J. Chem. Phys.*, 84 (1986) 5687–5705.
- [43] I.J.-H. Lii and N.L. Allinger, *J. Phys. Org. Chem.*, 7 (1994) 591–609.
- [44] N.L. Allinger and L. Yan, *J. Am. Chem. Soc.*, 115 (1993) 11918–11925.
- [45] A.D. French, L. Schäfer, and S.Q. Newton, *Carbohydr. Res.*, 239 (1993) 51–60.
- [46] A.D. French and M.K. Dowd, *J. Comp. Chem.*, 15 (1994) 561–570.
- [47] N.L. Allinger, X.F. Zhou, and J. Bergsma, *J. Mol. Struct. (Theochem)*, 118 (1994) 69–83.
- [48] C. Van Alsenoy, A.D. French, M. Cao, S.Q. Newton, and L. Schäfer, *J. Am. Chem. Soc.*, 116 (1994) 9590–9595.
- [49] M.K. Dowd, A.D. French, and P.J. Reilly, *Carbohydr. Res.*, 264 (1994) 1–19.
- [50] C.C. Chambers, G.D. Hawkins, C.J. Cramer, and D.G. Truhlar, *J. Phys. Chem.*, 100 (1996) 16385–16398.
- [51] M.J.S. Dewar, E.G. Zoebisch, E.F. Healy, and J.J.P. Stewart, *J. Am. Chem. Soc.*, 107 (1985) 3902–3909.
- [52] J.W. Storer, D.J. Giesen, C.J. Cramer, and D.G. Truhlar, *J. Comput.-Aid. Mol. Des.*, 9 (1995) 87–110.
- [53] J.W. Storer, D.J. Giesen, G.D. Hawkins, G.C. Lynch, C.J. Cramer, D.G. Truhlar, and D.A. Liotard, in C.J. Cramer and D.G. Truhlar (Eds.), *Structure and Reactivity in Aqueous Solution*, ACS Symposium Series 568, American Chemical Society, Washington, DC, 1994, pp 24–49.
- [54] D.A. Liotard, G.D. Hawkins, G.C. Lynch, C.J. Cramer, and D.G. Truhlar, *J. Comp. Chem.*, 16 (1995) 422–440.
- [55] C.J. Cramer and D.G. Truhlar, *Chem. Phys. Lett.*, 198 (1992) 74–80; 202 (1993) 1567(E).
- [56] M.J. Frisch, G.W. Trucks, H.B. Schlegel, P.M.W. Gill, B.G. Johnson, M.A. Robb, J.R. Cheeseman, T. Keith, G.A. Petersson, J.A. Montgomery, K. Raghavachari, M.A. Al-Laham, V.G. Zakrzewski, J.V. Ortiz, J.B. Foresman, J. Cioslowski, B.B. Stefanov, A. Nanayakkara, M. Challacombe, C.Y. Peng, P.Y. Ayala, W. Chen, M.W. Wong, J.L. Andres, E.S. Replogle, R. Gomperts, R.L. Martin, D.J. Fox, J.S. Binkley, D.J. DeFrees, J. Baker, J.P. Stewart, M. Head-Gordon, C. Gonzalez, and J.A. Pople, *GAUSS-IAN94 RevD.1*, GAUSSIAN Inc., Pittsburgh, PA, 1995.
- [57] E.D. Glendening, J.E. Carpenter, and F. Weinhold, *NBO version 3.1*, University of Wisconsin, Madison, WI, 1995.
- [58] G.D. Hawkins, G.C. Lynch, D.J. Giesen, I. Rossi, J.W. Storer, D.A. Liotard, C.J. Cramer, and D.G. Truhlar, *QCPE Bull.*, 16 (1996) 11–13.
- [59] C.J. Cramer and D.G. Truhlar, *J. Am. Chem. Soc.*, 113 (1991) 8305–8315, 9901(E).
- [60] C.J. Cramer and D.G. Truhlar, in O. Tapia and J. Bertrán (Eds.), *Solvent Effects and Chemical Reactivity*, Kluwer, Dordrecht, 1996, pp. 1–81.
- [61] C.J. Cramer and D.G. Truhlar, *J. Am. Chem. Soc.*, 113 (1991) 8552–8553 9901(E).
- [62] W.L. Jorgensen and J. Tirado-Rives, *J. Am. Chem. Soc.*, 110 (1988) 1657–1666.
- [63] W.L. Jorgensen, J. Chandrasekhar, J.D. Madura, R.W. Impey, and M.L. Klein, *J. Chem. Phys.*, 79 (1983) 926–935.
- [64] I. Tvaroška, *Biopolymers*, 21 (1982) 1887–1897.
- [65] C.J. Cramer, unpublished calculations.
- [66] C.J. Cramer and D.G. Truhlar, *J. Am. Chem. Soc.*, 116 (1994) 3892–3900.
- [67] S.E. Barrows, C.J. Cramer, D.G. Truhlar, E.J. Weber, and M.S. Elovitz, *Environ. Sci. Technol.*, in press.
- [68] W.F. van Gunsteren and H.J.C. Berendsen, *Groningen Molecular Simulation (GROMOS) Library Manual*, BIOMOS, Nijenbourgh 16, Groningen, The Netherlands, 1987.
- [69] K.-H. Ott and B. Meyer, *J. Comp. Chem.*, 17 (1996) 1068–1084.